

Comparing conditional autoregressive models for Bayesian spatial mapping of dengue cases in Indonesia

Ferra Yanuar,¹ Yudiantri Asdi,¹ Aidinil Zetra,² Sofiana Wudlu,¹ Fenni Kurnia Mutiya,³ Rahmawita,¹

¹Department of Mathematics and Data Science, Universitas Andalas; ²Department of Political Sciences, Universitas Andalas; ³Department of Statistics, Universitas Negeri Padang, Indonesia

Abstract

Dengue Haemorrhagic Fever (DHF) remains a public health burden in Indonesia with substantial provincial variation. We modelled province-level DHF counts in 2023 using Bayesian spatial conditional autoregressive Poisson models with population offsets. Predictors were average annual temperature (per 1°C) and the number of public health workers (province-level count). Spatial dependence was supported by Moran's $I=0.4689$ ($p=0.021$). We fitted models using Besag-York-Mollié (BYM) and Leroux priors via Markov chain Monte Carlo and compared fit using the Deviance Information Criterion (DIC) and the Watanabe-Akaike Information Criterion (WAIC). In the BYM model, temperature was associated with lower risk (RR=0.90; 95% CrI: 0.76 to 1.07), with uncertainty including unity, whereas workforce density was associated with higher reported risk (RR=1.05; 95% CrI: 1.03 to 1.07). Estimates were similar under the Leroux prior (temperature RR=0.89; 95% CrI: 0.74 to 1.07; workforce RR=1.04; 95% CrI: 1.02 to 1.07), and BYM showed marginally better fit. Risk mapping indicated elevated burden in parts of Kalimantan and eastern Indonesia. Findings may inform geographically targeted surveillance and vector control; the workforce association should be interpreted cautiously because it may reflect reporting capacity or reactive deployment.

Key words: dengue, spatial, Bayesian Spatial Conditional Autoregression, Besag-York-Mollié, Leroux, Indonesia.

Correspondence: Ferra Yanuar, Department of Mathematics and Data Science, Universitas Andalas, 25163, Indonesia.
E-mail: ferrayanuar@sci.unand.ac.id

Introduction

Dengue Haemorrhagic Fever (DHF) remains a major public health concern in Indonesia. As an archipelagic country with wide differences in climate, urbanisation and connectivity, Indonesia shows clear geographic differences with regard to dengue burden (Aswi *et al.*, 2020). Provinces can vary greatly in incidence within the same year, so a uniform, 'one size fits all' control approach can spread efforts too thin in high-risk areas and spend too much where risk is lower.

Risk mapping helps turning routine surveillance counts into practical signals for decision-makers. In Indonesia, two research gaps remain: the geographic and the methodological one. First, national scale dengue risk maps that allow direct comparison across all provinces within one consistent modelling framework are still limited. Many studies focus on selected regions, particular cities or short time periods, so they do not support prioritisation across provinces. Second, even when spatial models are used, studies rarely check how sensitive the risk pattern is to the choice of Conditional Autoregressive (CAR) priors (spatial smoothing assumptions). This is important because different CAR choices can lead to different levels of smoothing, different views of clustering, and different uncertainty, which can affect which provinces are labelled "high risk" for policy action (Franco-Villoria *et al.*, 2022). This study addresses both gaps using a national scale modelling

setup designed for a fair, like for like comparison. We analysed dengue case counts from all 34 Indonesian provinces in 2023 using a Bayesian hierarchical Poisson model with a population offset, and we produced province specific estimates of relative risk using the same data structure and covariates. Spatial dependence was modelled using two widely used CAR specifications, the Besag-York-Mollié (BYM) model and the Leroux model (Lee, 2011), fitted with identical covariates and estimation settings. The key methodological feature is that we keep the data, covariates and other model parts the same, so any differences in the national risk maps can be linked to the CAR choice rather than to changes in inputs or model components (Lee *et al.*, 2018).

The outputs include province level posterior relative risk estimates, credible intervals (Bayesian uncertainty ranges) and probability-based flags such as the posterior probability that relative risk exceeds 1 (Jaya *et al.*, 2023). These outputs support practice in three concrete ways. For targeted surveillance, provinces with high estimated risk and high exceedance probability can be prioritised for stronger case finding, reporting checks and expansion of sentinel sites, while wide uncertainty can indicate where surveillance needs to be strengthened before major operational changes are made (Nazia *et al.*, 2022). For vector control, the maps help focus larval source management and adult mosquito control in provinces that show consistently higher risk under both CAR priors, which offers a practical definition of "robust priority areas." For resource

allocation, risk and uncertainty together can guide how diagnostics, outbreak response teams and workforce capacity are deployed, and also support transparent decisions by showing where evidence is strong and where it remains uncertain. In this way, the study provides a nationally comparable risk map for Indonesia and an explicit sensitivity check that shows how stable policy relevant conclusions are under different CAR priors (Palmi-Perales *et al.*, 2021; Yanuar, Abrari, Zetra, *et al.*, 2023).

Materials and Methods

Data and study area

This cross-sectional ecological study covered all 34 provinces of Indonesia using 2023 data. The primary outcome was the annual number of dengue cases in province i (Y_i), aggregated from the monthly national dengue surveillance database of the Ministry of Health. Population projections for 2023 from Statistics Indonesia were used to compute expected cases via indirect standardisation: $E_i = P_i \times r$, where P_i is the projected population and $r = \sum_i Y_i / \sum_i P_i$ is the national 2023 incidence rate. In the Poisson log-linear model, $\log(E_i)$ was included as an offset with its coefficient fixed at 1. Prior to model fitting, we evaluated collinearity between the covariates using the Variance Inflation Factor (VIF); a diagnostic that measures how much the variance of a regression coefficient is inflated due to correlations among predictors. We used a rule-of-thumb threshold of $VIF > 5$ to indicate potentially problematic multicollinearity. Two key covariates were selected based on their established relevance in dengue epidemiology. First, the average annual temperature ($^{\circ}\text{C}$) was included as a proxy for environmental suitability for the *Aedes aegypti* vector, with data obtained from the Meteorological, Climatological and Geophysical Agency (BMKG) of Indonesia (<http://wis.bmkg.go.id/openwis-user-portal/srv/en/about.home>). Second, the number of public health workers (province-level count) was included as a proxy for surveillance and reporting capacity across provinces. This variable was derived from the Ministry of Health's annual health profile report. The spatial framework was delineated using a digital polygon map of the 34 provincial boundaries. The detail descriptive statistics about these candidate variables are presented in Table 1. From Table 1, it is apparent that the mean of DHF cases for 2023 in all provinces in Indonesia was 3,644 cases. Gorontalo Province had the lowest number of cases (683) and West Java Province the highest (19,328).

Spatial dependency assessment

To formally quantify the degree of spatial clustering in dengue case, a preliminary spatial analysis was performed. A spatial weights matrix (W) was constructed based on a first-order queen contiguity criterion, where two provinces were considered neighbours if they shared a common border or vertex (Jaya *et al.*, 2023; Yanuar, Abrari, Hg, 2023). This binary matrix was then row-standardized to ensure that the weights for each province summed to one (Lee, 2011). We then calculated the global Moran's I statistic to test the null hypothesis of spatial randomness in the Standardised Incidence Ratios (SIRs) of DHF across provinces (Lee *et al.*, 2018). A statistically significant and positive Moran's I value would confirm the presence of positive spatial autocorrelation, thereby justifying the application of spatial regression models (Leroux *et al.*, 2000; Yanuar, Abrari, Rahmi, Zetra, 2023).

Bayesian spatial modelling framework

In spatial regression, residual spatial autocorrelation often arises when observations are geographically dependent, violating the independence assumption of classical regression. Such correlation typically results from environmental effects (units influenced by neighbouring areas) or grouping effects (similar units clustering together) (Aswi, Cramb, Duncan, *et al.*, 2020; MacNab, 2022).

To model the provincial DHF case counts while accounting for spatial dependence, we employed a Bayesian Spatial Conditional Autoregressive (BSCAR) framework. The observed number of DHF cases (y_i) in each province i was assumed to follow a Poisson distribution, conditioned on an expected number of cases (E_i) and a relative risk (θ_i) (MacNab, 2022; Sukarna *et al.*, 2025; Yanuar *et al.*, 2025).

Offset formulation: We parameterised the Poisson mean as $\mu_i = E_i r_i$, where r_i is the province-specific relative risk. Equivalently, the linear predictor can be expressed as $\log(\mu_i) = \log(E_i) + \alpha + \beta_1 x_{i1} + \beta_2 x_{i2} + \varphi_i$, so $\log(E_i)$ enters the model as an offset with its coefficient fixed at 1. This adjustment accounts for population size differences across provinces, so covariate and spatial effects capture departures from the national baseline risk.

$$y_i \sim \text{Poisson}(E_i \theta_i), \quad (\text{Eq. 1})$$

for the i^{th} area, $i = 1, \dots, n$. The model was specified on the log scale as follows:

$$\ln(\theta_i) = \beta_0 + \beta_1 X_{i1} + \beta_2 X_{i2} + \psi_i \quad (\text{Eq. 2})$$

where β_0 represents the overall log relative risk for the entire study area; x_{i1} and x_{i2} are the province specific covariates (temperature and health worker density, respectively); β_1 and β_2 their corresponding regression coefficients; ψ_i a spatial random effect that captures latent, unobserved spatial heterogeneity not explained by the covariates (Yanuar *et al.*, 2023). This component is crucial for borrowing strength from neighbouring provinces to produce more stable and reliable risk estimates, a hallmark of modern disease mapping (Leroux *et al.*, 2000). The formulation above allows the model to capture both fixed effects of covariates and latent spatial processes that may drive clustering in disease risk, thereby improving the accuracy and interpretability of risk estimates in spatial epidemiology.

Conditional autoregressive (CAR) priors

We compared two distinct prior specifications for the spatial random effect term, ψ_i , which are prominent in the spatial epidemiology literature: the BYM model and the Leroux CAR model.

The BYM model is a widely adopted specification that decomposes the spatial random effect, ψ_i , into two components:

$$\psi_i = u_i + v_i \quad (\text{Eq. 3})$$

where u_i represents a spatially structured effect, which captures spatial correlation among neighbouring provinces and is assigned an Intrinsic CAR (ICAR) prior (Nazia *et al.*, 2022) and an unstructured random effect, assumed to be independent and identically distributed (*e.g.*, $v_i \sim N(0, \sigma_v^2)$), which accounts for non-spatial heterogeneity or overdispersion (MacNab, 2022). This dual component structure provides a flexible approach to modelling different sources of variation in disease risk (Palmi-Perales *et al.*, 2021).

This model has been applied extensively to binomial, Poisson and zero-inflated Poisson data, particularly in disease mapping studies, due to its ability to capture heterogeneity across regions (Lee *et al.*, 2018). The hypotheses model for CAR BYM model is as presented in Eq. (3). An ICAR prior was assigned to β_j , such that

$$(u_i | u_j, i \neq j, \sigma_u^2) \sim N\left(\frac{\sum_j u_j w_{ij}}{\sum_j w_{ij}}, \frac{\sigma_u^2}{\sum_j w_{ij}}\right) \tag{Eq. 4}$$

where the variance components σ_u^2 and σ_v^2 were endowed with weakly informative priors, specified as InverseGamma distributions (1, 0.01), consistent with the default hyperprior parameterization implemented in CARBayes.

To improve flexibility, Leroux *et al.* (2000) proposed an alternative CAR specification with a spatial dependence parameter, ρ , bounded between 0 and 1. When ρ approaches 1, strong spatial correlation is present, resembling the BYM model, while values near 0 indicate little to no spatial dependence. This formulation provides more stable parameter estimation and improved interpretability compared to BYM, particularly for health applications.

While the BYM CAR model incorporates two distinct random effect components, the Leroux specification employs only a single spatial random effect, u_i . The hypothesis model for Leroux CAR model is presented by:

$$\psi_i = u_i$$

$$(u_i | u_j, i \neq j, \sigma_u^2) \sim N\left(\frac{\rho \sum_j u_j w_{ij}}{\rho \sum_j w_{ij} + 1 - \rho}, \frac{\sigma_u^2}{\sum_j w_{ij}}\right) \tag{Eq. 5}$$

where hyperpriors are given by $\sigma_u^2 \sim \text{InversGamma}(1, 0.01)$ and $\rho \sim \text{Uniform}(0, 1)$.

Model implementation and comparison

Posterior inference for all models was conducted using Markov Chain Monte Carlo (MCMC) simulation, implemented in R software with the CARBayes package (Lee, 2013). Vague (diffuse) normal priors were assigned to all fixed effect coefficients (β_2), while the standard Inverse-Gamma (1, 0.01) hyperpriors were specified for the variance components. Two parallel MCMC chains were run with 500,000 iterations, following a burn-in period of 100,000 iterations, applying a thinning interval of 200 to reduce autocorrelation in the posterior samples. Model convergence was assessed through visual inspection of trace plots and by ensuring the Gelman-Rubin diagnostic (Brooks & Gelman, 1998). Model performance and fit were rigorously compared using the Deviance Information Criterion (DIC) and the Watanabe-Akaike Information Criterion (WAIC). Both criteria balance model fit against complexity, with lower values indicating a more parsimonious and better-fitting model. The model with the superior fit was subsequently used for generating the final spatial risk estimates.

Results

Before presenting the model-based risk estimates, we first summarised the observed provincial distribution of dengue incidence and its bivariate patterns with key environmental variables. This descriptive overview provides context for the subsequent spatial modelling results and helps clarify where the raw burden is concentrated in the 2023 cross-section.

Figure 1 shows that the DHF incidence was highest in Kalimantan, led by Central Kalimantan (about 174 cases per 100,000), followed by West Kalimantan (about 160), East Kalimantan (about 143), and North Kalimantan (about 135). North

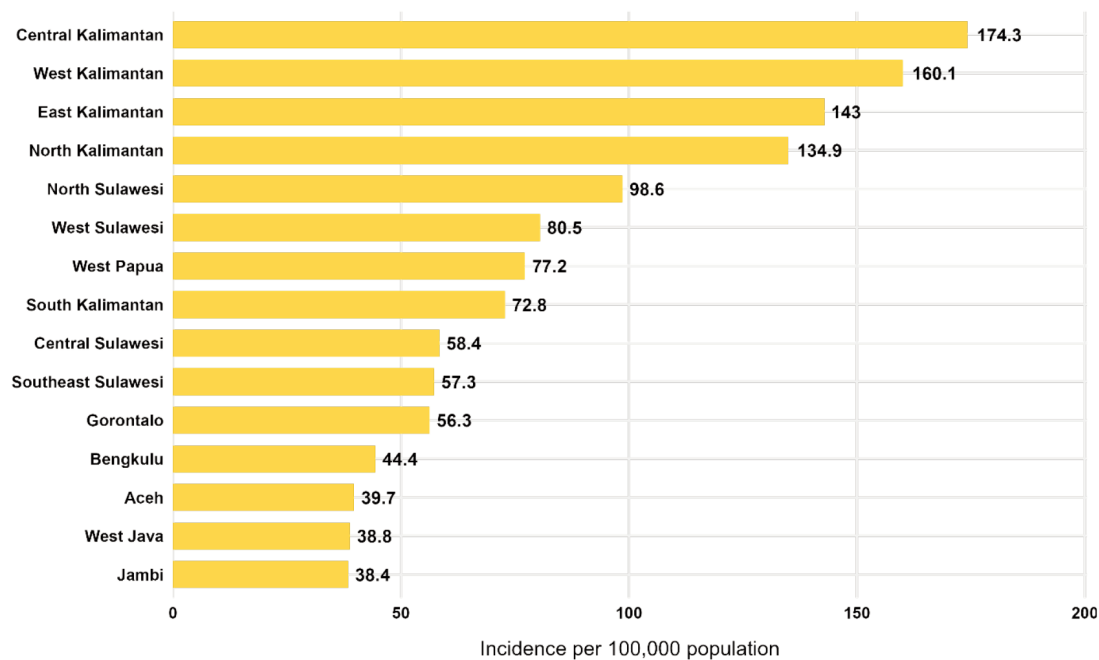


Figure 1. Dengue incidence for the top 15 provinces in Indonesia in the year 2023.

Sulawesi was the next highest province, remaining below 100 per 100,000. Several populous provinces recorded large absolute case counts but moderate incidences; for example, West Java had the largest number of cases but an incidence of around 39 per 100,000, while Jakarta was about 37 per 100,000.

Figure 2a indicates a moderate negative bivariate association between average temperature and dengue incidence in this cross-section. This pattern should be interpreted cautiously because rainfall alone may not capture key drivers of transmission, including water storage practices, urban density, housing conditions, and local vector control. Figure 2b shows little evidence of a positive relationship between average temperature and incidence across provinces in 2023.

To ensure that subsequent regression estimates were not compromised by strong correlations among predictors, we screened the covariates for collinearity using VIF, which quantify the extent to which predictor correlations inflate coefficient uncertainty. The VIF values were essentially 1 for both predictors, with the average annual temperature (X_1)=1.000194 and the number of public health workers (X_2)=1.000194, indicating negligible collinearity and virtually no inflation of coefficient variance. Thus, the estimated covariate effects were unlikely to be distorted by multicollinearity. Beyond covariate relationships, the dengue incidence may also exhibit geographic clustering that cannot be captured by non-spatial models. Accordingly, we tested spatial dependence using Moran's I , which in this study was 0.4689 with $p=0.021$ ($\alpha=0.05$), indicating statistically significant spatial autocorrelation across provinces and motivating the use of spatial random effects.

Model BSCAR DHF cases in Indonesia

We fitted Bayesian spatial conditional autoregressive (CAR) models and report results under the two common priors: BYM and Leroux. Parameter estimates based on BSCAR BYM model are presented in Table 2.

Based on the estimated model provided in Table 2, the proposed model based on BSCAR BYM was the following:

$$\ln(\widehat{\mu}_i) = 9.7589 - 0.1054X_1 + 0.0005X_2 + \psi_i, \quad (\text{Eq. 6})$$

The BSCAR BYM model revealed several important determinants of dengue incidence across the Indonesian provinces. The estimated coefficient for the average annual temperature (X_1) was negative (-0.1054) suggesting a 10% reduction in dengue incidence for each one-degree Celsius increase after adjusting for other covariates. However, the 95% Credible Interval (CI) included zero implying that this association was not statistically significant within the model's uncertainty range. In contrast, the number of public health workers (X_2) exhibited a small but statistically significant positive effect (0.0005) corresponding to an approximate 0.05% increase in the mean number of cases per additional health worker. This finding should be interpreted cautiously as it likely reflects a reactive allocation of health resources to high-burden provinces rather than a causal effect whereby additional health workers increase case counts, a phenomenon consistent with reverse causality. The structured spatial variance was noticeably larger than the unstructured variance indicating that a substantial share of residual heterogeneity was spatially correlated rather than independent noise.

Estimation under the BSCAR Leroux model (Table 3) yielded comparable results, with the health worker variable again positively associated with dengue risk. The spatial dependence parameter ρ was estimated at approximately 0.68, indicating moderate spatial correlation across provinces. This supports the interpretation that dengue risk in Indonesia is shaped by both local conditions and regional spillover effects.

Based on the parameter estimates reported in Table 3, the proposed model under the BSCAR Leroux specification can be expressed as follows:

$$\ln(\widehat{\mu}_i) = 10.2593 - 0.1114X_1 + 0.0004X_2 + \psi_i, \quad (\text{Eq. 7})$$

The results of the Bayesian spatial Leroux model demonstrate a clear and statistically significant spatial structure in dengue incidence across Indonesian provinces. The estimated coefficient for average annual temperature (X_1)= -0.1114) suggests a negative association with dengue incidence, implying roughly a 10% reduction in expected cases per one-degree Celsius increase, although the

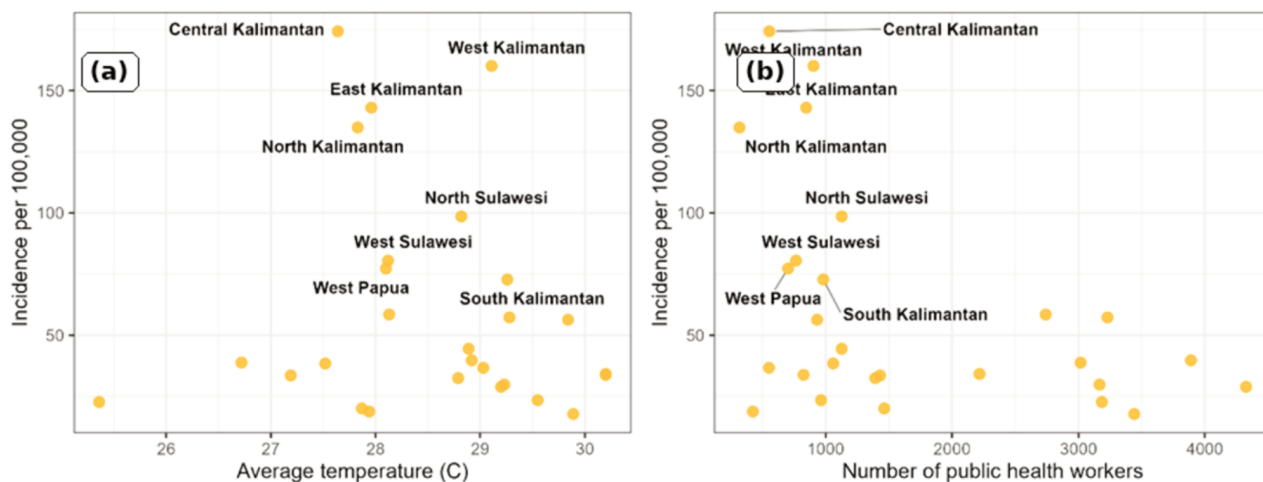


Figure 2. DHF incidence in relation to temperature and the number of public health workers by province in the year 2023.

95% CI includes zero, which indicates that this effect is not statistically conclusive. In contrast, the number of public health workers ($X_2 = 0.0004$) was positively and significantly associated with dengue incidence, although the magnitude was small (about 0.04% per additional worker). This result is best interpreted as evidence of a reactive allocation of health resources to high-burden areas rather than a causal driver of increased case counts. The posterior mean of the spatial variance component ($\sigma_u^2 = 0.5451$) confirms substantial spatial heterogeneity, and the spatial dependence parameter ($\rho = 0.6946$) indicates moderate-to-strong spatial autocorrelation, suggesting that neighbouring provinces exhibited correlated risk patterns. Collectively, these findings highlight the importance of spatially explicit modelling for accurately characterizing disease risk and support geographically targeted surveillance and intervention strategies.

Model fit was compared using both DIC and WAIC, where smaller values indicate better expected out-of-sample performance. The BYM specification yielded marginally lower DIC and WAIC than the Leroux specification (DIC: 316.87 vs 317.50; WAIC: 309.84 vs 310.66). However, the absolute differences were very small (less than 1 point for both criteria) indicating that the two CAR priors provide essentially comparable fit for these data. Therefore, substantive conclusions about spatial risk patterns and covariate associations were unlikely to be sensitive regardless which approach was used, and the choice between BYM and Leroux can reasonably be guided by interpretability and reporting

preference rather than fit alone. This result is broadly consistent with the parameter estimates reported earlier, where both models produced similar covariate effects and confirmed the presence of significant spatial heterogeneity. The slightly better performance of the BYM specification may reflect its ability to decompose spatial random effects into structured (u_i) and unstructured (v_i) components, thereby providing a more flexible representation of residual variability. Nevertheless, the difference between the two models was relatively small indicating that both models adequately capture the spatial dependence structure. For policy and communication purposes, the Leroux model remains attractive due to its parsimony and interpretability, even if the BYM model exhibits a minor advantage in terms of information criteria.

Spatial risk estimates

Province-specific risk was summarised using the Standardised

Incidence Ratio (SIR), defined as $SIR_i = \frac{O_i}{E_i}$, where O_i is the observed number of cases and E_i is the expected number of cases from indirect standardisation. Values above 1 indicate higher-than-expected risk relative to the national baseline. Using the best-fitting BYM model, province-specific SIRs were estimated and presented in Table 4. Elevated risks were observed in several provinces of the Kalimantan region (e.g. Central, East and North Kalimantan), where the SIR values exceeded 3.5, indicating more

Table 1. Descriptive statistics of the variables.

Variable	Mean	Minimum	Q1	Median	Q3	Maximum
Number of DHF case (Y)	3,644	683	1,302	2,181	4,366	19,328
Average annual temperature (X_1)	28.54	25.36	27.91	28.82	29.25	30.20
Number of public health workers (X_2)	1,687.9	318	835.5	1126	2879	4326

DHF, dengue haemorrhagic fever; Q_1 and Q_3 denote the first and third quartiles, representing the 25th and 75th percentiles of the distribution, respectively. These statistics help describe the variability and distributional pattern of the observed values across provinces.

Table 2. Parameter estimated for number of DHF cases using the BSCAR BYM model.

Variable	Estimated Mean	Lower Bound	Upper Bound
Intercept	9.7589*	4.7485	14.5776
Average annual temperature (X_1)	-0.1054	-0.2749	0.0703
Number of public health workers (X_2)	0.0005*	0.0003	0.0007
σ_u^2	0.5266*	0.0458	1.0351
σ_v^2	0.0310*	0.0023	0.2603

*Posterior probability of the coefficient being above (or below) 0 exceeds 0.95.

Table 3. Parameter estimated for number of dengue risk using BSCAR Leroux Model.

Variable	Estimated Mean	Lower Bound	Upper Bound
Intercept	10.2593*	5.2154	15.6498
Average annual temperature (X_1)	-0.1114	-0.3027	0.0671
Number of public health workers (X_2)	0.0004*	0.0002	0.0007
σ_u^2	0.5451*	0.3081	0.9540
ρ	0.6946*	0.3317	0.9246

*Posterior probability of the coefficient being above (or below) 0 exceeds 0.95.

than threefold higher dengue incidence compared with expectation. These provinces, characterized by rapid urban expansion, environmental change, and uneven health infrastructure, appear particularly vulnerable. Other provinces such as Bengkulu, West Java and South Kalimantan also displayed excess risk, though at more moderate levels (SIR between 1.0 and 2.0). Conversely, provinces in Java (Central Java, Yogyakarta, East Java) and Lampung exhibited lower-than-expected risk ($SIR < 0.6$).

Discussion

The observed spatial clustering suggests that geographically targeted strategies are appropriate. Provinces with consistently high SIRs can be prioritised for intensified vector control, environmental management, and community-based prevention. The positive association between health worker density and reported cases should be interpreted as a signal of surveillance and reporting capacity, or resource allocation responding to burden, rather than evidence of causation. This implies that comparisons of incidence across provinces should consider potential differences in detection and reporting alongside true transmission risk.

These findings presented here align with previous Bayesian spatial analyses in Southeast Asia, which consistently demonstrate that dengue risk is unevenly distributed and strongly influenced by both ecological and health system factors (Aswi *et al.*, 2020; Jaya *et al.*, 2021; MacNab, 2022). This study provides, to our knowledge, one of the first province-level Bayesian spatial dengue risk maps for Indonesia at the national scale, alongside a like-for-like sensitivity assessment to alternative CAR priors.

This study is ecological, using province-level aggregates for a single year, so individual-level causal inference is not supported and ecological bias is possible. Reported case counts may be affected by underreporting and heterogeneous surveillance quality across provinces, which could partly explain the positive association with health worker density. In addition, the covariate set was restricted and measured at coarse spatial and temporal resolution, so important drivers such as urbanisation intensity, housing and water storage practices, mobility, land use, and entomological indices were not directly captured. Future work should extend to multi-year spatio-temporal modelling, incorporate richer socio-environmental and health-system covariates, evaluate alternative adjustments for reporting completeness and, where feasible, move to finer geographic units to support more operational targeting.

Table 4. Estimate for Standardised Incidence Ratios (SIRs).

No.	Province	\hat{Y}_i	E_i	SIR_i
1	Aceh	2178.65	2105.06	1.03*
2	North Sumatera	4576.97	5907.83	0.77
3	West Sumatera	1928.51	2210.53	0.87
4	Riau	2152.36	2550.61	0.84
5	Jambi	1413.66	1412.66	1.00*
6	South Sumatera	2982.64	3357.15	0.88
7	Bengkulu	929.20	800.94	1.16*
8	Lampung	2179.87	3576.20	0.60
9	DKIJakarta	3907.91	4097.65	0.95
10	West Java	19325.02	19144.36	1.01*
11	Central Java	6660.01	14414.24	0.46
12	DIYogyakarta	702.45	1434.66	0.46
13	East Java	9399.26	15945.05	0.58
14	Banten	4153.74	4725.66	0.87
15	West Kalimantan	9001.30	2159.12	4.16*
16	Central Kalimantan	4833.17	1064.99	4.53*
17	South Kalimantan	3073.42	1621.19	1.89*
18	East Kalimantan	5589.83	1501.16	3.72*
19	North Kalimantan	987.92	280.29	3.52*
20	North Sulawesi	2640.29	1029.58	2.56*
21	Central Sulawesi	1803.83	1185.20	1.52*
22	South Sulawesi	2702.16	3594.74	0.75
23	Southeast Sulawesi	1574.92	1055.51	1.49*
24	Gorontalo	684.70	465.82	1.46*
25	West Sulawesi	1190.33	568.68	2.09*
26	Papua	897.67	1721.17	0.52
27	West Papua	916.43	455.87	2.01*

*high risk ($SIR > 1$)

References

- Anselin L, 1988. The scope of spatial econometrics. In L. Anselin, Spatial Econometrics: Methods and Models (Vol. 4, pp. 7–15). Springer Netherlands.
- Anselin L, 2009. Spatial regression. In A. S. Fotheringham & P. A. Regerson (Eds.), The Sage Handbook of Spatial Analysis (pp. 225–276). SAGE Publications Ltd.
- Aswi A, Cramb S, Duncan E, Hu W, White G, Mengersen K, 2020. Bayesian Spatial survival models for hospitalisation of dengue: a case study of Wahidin Hospital in Makassar, Indonesia. *Int J Environ Res Public Health* 17:878.
- Brooks S, Gelman A, 1998. General methods for monitoring convergence of iterative simulations. *J Comput Graph Stat* 7:434–55.
- Franco-Villoria M, Ventrucci M, Rue H. 2022. Variance partitioning in spatio-temporal disease mapping models. *Stat Methods Med Res* 31:1566–78.
- Jaya I, Andriyana Y, Tantular B, 2021. Spatial prediction of malaria risk with application to Bandung City, Indonesia. *IAENG Int J Appl Math* 51:1-22.
- Jaya I, IGNM, Chadidjah A, Kristiani F, Darmawan G, Princidy, JC. 2023. Does mobility restriction significantly control infectious disease transmission? Accounting for non-stationarity in the impact of COVID-19 based on Bayesian spatially varying coefficient models. *Geospat Health*, 18:1161
- Lee D, 2011. A comparison of conditional autoregressive models used in Bayesian disease mapping. *Spat Spatio-Temporal Epidemiol* 2:79–89.
- Lee D. 2013. CARBayes: an R package for Bayesian spatial modeling with conditional autoregressive priors. *J Statistical Software* 55:i13.
- Lee, D, Rushworth A, Napier G, 2018. Spatio-temporal areal unit modeling in R with conditional autoregressive priors using the CARBayesST Package. *J Stat Softw* 84:1-39.
- Leroux BG, Lei X, Breslow N, 2000. Estimation of disease rates in small areas: a new mixed model for spatial dependence. In M. E. Halloran & D. Berry (Eds.), *Statistical Models in Epidemiology, the Environment, and Clinical Trials* (Vol. 116, pp. 179–191). Springer New York.
- MacNab YC, 2022. Bayesian disease mapping: Past, present, and future. *Spat Stat* 50, 100593.
- Nazia N, Law J, Butt ZA2022. Identifying spatiotemporal patterns of COVID-19 ansmissons and the drivers of the patterns in Toronto: A Bayesian hierarchical spatiotemporal modelling. *Sci Rep* 12:9369.
- Palmi-Perales F, Gómez-Rubio V, Martínez-Beneito MA, 2021. Bayesian multivariate spatial models for lattice data with INLA. *J Stat Softw* 98:1-29.
- Sukarna S, Wijayanto H, Angraini Y, Kurnia A, 2025. A Bayesian spatiotemporal Poisson conditional autoregressive model for dengue haemorrhagic fever in Indonesia integrating satellite-generated environmental data. *Geospat Health* 20:1379.
- Yanuar F, Abrari, T Hg IR, 2023. The construction of unemployment rate model using SAR, quantile regression, and SARQR model. *Pak J Stat Oper Res* 19:447–58.
- Yanuar F, Abrari T, Izzati Rahmi HG Zetra A, 2023. Spatial autoregressive quantile regression with application on open unemployment data. *Sci Technol Indones* 8:321–29.
- Yanuar F, Abrari T, Zetra A, Izzati Rahmi HG, Devianto D, Ahda S, 2023. Examining regional factors on malnutrition rate in Indonesia using spatial autoregressive approach. *Commun Math Biol Neurosci* 60:1–21.
- Yanuar F, Wulandari S, Asdi Y, Zetra A, Haripamyu, 2025. Modeling of human development index using Bayesian spatial autoregressive approach. *Sci Technol Indones* 10:72–9.

Received: 19 September 2025; Accepted: 25 March 2026.

Contributions: Ferra Yanuar: conceptualization, methodology, formal analysis, software, data curation, writing original draft preparation, supervision. Yudiantri Asdi: methodology, validation, formal analysis, writing review and editing. Aidinil Zetra: interpretation of results, public health policy interpretation, writing review and editing. Sofiana Wudlu: data curation, investigation, visualization, writing review and editing. Fenni Kurnia Mutiyya: statistical validation, methodology, writing review and editing. Rahmawita: data collection, data preparation, literature review, investigation, and writing support. All authors have read and approved the final manuscript.

Conflict of interest: the authors declare no potential conflict of interest, and all authors confirm the accuracy and integrity..

Ethics approval: this study used secondary aggregated province-level surveillance and publicly available administrative data, with no individual identifiable human participant data. Therefore, formal ethical approval was not required

Availability of data and materials: all data generated or analyzed during this study are included in this published article.

Acknowledgments: the authors would like to acknowledge Universitas Andalas for its support under the Penelitian Unggulan Jalur Kepakaran (PUJK) scheme (Contract No. 376/UN16.19/PT.01.03/PUJK/2025).

Funding: this research was supported by Universitas Andalas under the Penelitian Unggulan Jalur Kepakaran (PUJK) scheme (Contract No. 376/UN16.19/PT.01.03/PUJK/2025).

Publisher's note: all claims expressed in this article are solely those of the authors and do not necessarily represent those of their affiliated organizations, or those of the publisher, the editors and the reviewers. Any product that may be evaluated in this article or claim that may be made by its manufacturer is not guaranteed or endorsed by the publisher.

This work is licensed under a Creative Commons Attribution-NonCommercial 4.0 International License (CC BY-NC 4.0).